ACS OMEGA

http://pubs.acs.org/journal/acsodf

Article

Experimental Study on the Effect of CO_2 Injection Pressure on the Migration Characteristics and Extraction Effects of Replacement CH_4

Zhihao Fu, Baoshan Jia,* Yanming Wang, and Weipeng Tian

Cite This: *ACS Omega* 2023, 8, 28583−28591

Read Online

ACCESS | Metrics & More | Article Recommendations

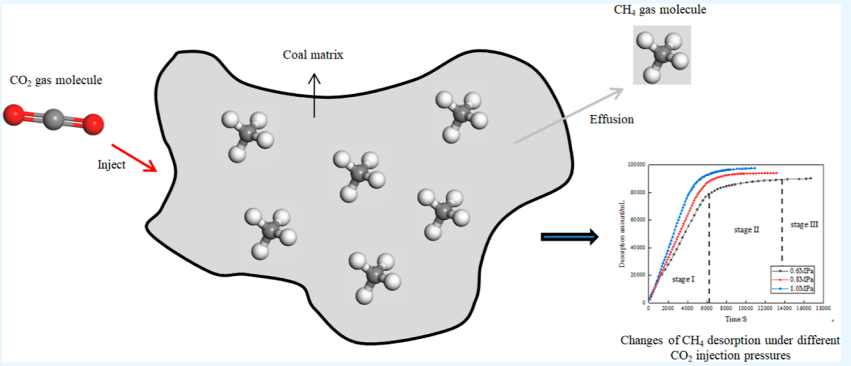

ABSTRACT: To study the effect of CO_2 injection pressure on gas migration characteristics and coalbed methane (CBM) extraction, a platform for the experimental replacement of CH_4 with CO_2 was used to conduct experiments on the replacement of CH_4 under different CO_2 injection pressures and analyze the gas transport characteristics and CH_4 extraction during the experiment. The results reveal that the rate of gas migration out of the coal seam accelerates with increasing gas injection pressure, as determined by comparisons of the migration rates between adjacent monitoring points. The change trend of the CH_4 desorption rate under different gas injection pressures is divided into slow decline, sharp decline, and stability stages, and the maximum value of the effective diffusion coefficient increases from 2.3×10^{-5} to 3.4×10^{-5} and 4.6×10^{-5} cm^2/s as the gas injection pressure increases from 0.6 to 0.8 and 1.0 MPa. Similarly, the change pattern of coal seam permeability can be divided into slow decline, sharp decline, and stability stages. After the gas injection pressure was increased from 0.6 to 0.8 and 1.0 MPa, the CH_4 desorption volume increased from 90.2 to 94.1 and 97.8 L, whereas the coal seam CO_2 sequestration volume increased from 269.2 to 274.2 and 322.8 L, respectively. In contrast, the CH_4 extraction efficiency increased from 76.9 to 80.2 and 82.9%, respectively. The research results have important reference value and practical significance for optimizing the CO_2 injection pressure and improving the CBM extraction.

1. INTRODUCTION

Energy is crucial to human life and greatly influences the world economy; however, the supply of traditional fossil energies such as oil and natural gas is under severe threat. According to BP's Energy Outlook, the consumption of natural gas as a major energy source has increased by 74% over the last 20 years and will continue to be a major source of energy in the future.[1] Conventional fossil fuels have prominent drawbacks; they release large amounts of CO_2 when used, which places a huge strain on the ecological environment.[2,3] Therefore, countries globally have adopted different methods to address the increasingly serious greenhouse effect.[4,5] Research has revealed that CO_2 capture and storage and CO_2-enhanced coal bed methane mining can effectively control CO_2 emissions.[6,7] Coalbed methane (CBM) is an important component of unconventional natural gas that can replace fossil energy, making it of great significance in reducing CO_2 emissions and mitigating the greenhouse effect. The strong adsorption capacity of the coal seam for CO_2 means that it can compete with CH_4 for adsorption and displace CH_4 from the coal seam, thus improving the efficiency of CH_4 extraction from the coal seam and achieving geological storage of CO_2.[8,9] China's coal reserves are large, with numerous CBM resources. Therefore, the effective enhancement of CBM production should be investigated.

In recent years, many scholars at home and abroad have conducted extensive research on the mechanism of the CO_2 injection for CH_4 replacement, and they have analyzed the

Received: May 2, 2023
Accepted: July 11, 2023
Published: July 24, 2023

desorption and diffusion of gas during replacement and obtained meaningful research results.[10,11] The injection of CO_2, N_2, or a mixture of CO_2/N_2 into coal seams can improve the gas production efficiency of CBM.[12−16] The pore space of the coal seam generates a pressure potential difference after CO_2 injection. This can increase the desorption rate of CH_4 in the coal seam, which has a strong adsorption capacity for CO_2, and the use of CO_2 to replace CH_4 can improve the CH_4 extraction rate and reduce the residual CH_4 in the coal seam.[17−19] Numerous scholars have experimentally investigated CO_2 injection to improve the CBM recovery rate.[20−22] Tu and Tang et al.[23,24] studied binary gas adsorption and desorption patterns in coal seams and concluded that CO_2 concentration gradually increases and CH_4 concentration gradually decreases during desorption, and the coal seam has a stronger adsorption capacity for CO_2. Long, Liu, and An et al.[25−27] studied the diffusion properties of multigases in coal seams and found their diffusion to be diverse. Yang et al.[28] studied different pressures and gases to remove CH_4 from coal seams and concluded that the duration required for CO_2 to escape the coal seam shortens with the increase in gas injection pressure, proving that increasing the gas injection pressure is beneficial for improving the CH_4 extraction efficiency. Wu et al.[29] used a self-developed triaxial desorption and adsorption test platform to analyze the mechanical properties and gas permeability experimentally and concluded that a higher CO_2 injection pressure lowers the strength and elastic modulus of the coal body. Yang et al.[30] found the replacement effect to dominate at the beginning of CO_2 injection to replace CH_4, which gradually shifted to a repelling effect. Jing et al.[31] studied the influence of different factors on the replacement of CH_4 by CO_2 and determined that the injection temperature of CO_2 is directly proportional to the replacement efficiency, whereas the water content is inversely proportional to the replacement efficiency. Zhou et al.[32] analyzed the replacement efficiency under multifactor coupling and concluded that the replacement efficiency increased with the injection pressure and injection temperature, whereas it decreased when the water content increased. Meng et al.[33] combined molecular simulations with methane desorption experiments to analyze the effect of the water content on the methane desorption rate and concluded that the greater the water content in a coal seam, the slower the methane desorption rate.

The influence of gas migration characteristics on CH_4 replacement in coal seams with different CO_2 injection pressures has not been sufficiently studied. Therefore, three sets of experiments were conducted at different injection pressures to record data during experiments on the replacement of CH_4 with CO_2 in real time. The CH_4 migration rate, CH_4 desorption rate, CH_4 effective diffusion coefficient, and coal seam permeability were accurately recorded during the replacement of CH_4 with CO_2 to analyze the gas migration characteristics and CH_4 extraction effect during replacement at different pressures.

2. EXPERIMENTAL METHODS

2.1. Experimental Theoretical Analysis. During the CO_2 injection to replace CH_4 in coal seams, binary gases compete for adsorption, resulting in CH_4 gas escaping from coal seams through desorption−diffusion−percolation. The characteristics of gas transport in the pores, fractures, and coal matrix of the coal seam during gas injection replacement are shown in Figure 1.

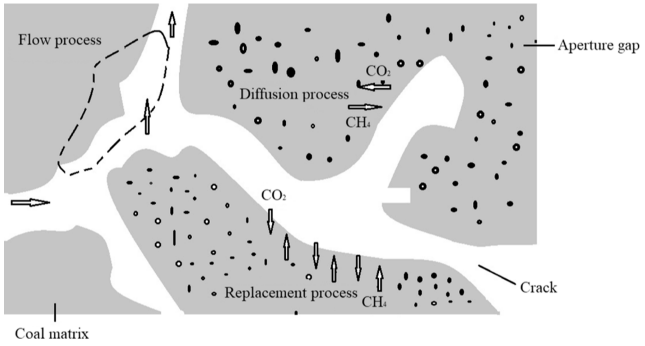

Figure 1. Gas migration characteristics during CO_2 replacement of CH_4.

After CO_2 injection, the free-state CH_4 gas in the coal seam fissure is channeled out of the coal seam under seepage action, and the CH_4 content in the coal seam pore fissure continually decreases, whereas the CH_4 pressure continually decreases. Gas diffusion commences after CH_4 is discharged from the pore fissures of the coal seam, and the adsorbed CH_4 gas molecules within the coal matrix diffuse outward. The CH_4 gas molecules on the surface of the coal seam pore fissures then begin to desorb into the fissure channels to escape from the coal seam via displacement.[34−36] The gas injected into the coal seam to expel CH_4 is subject to the joint action of desorption−diffusion−percolation, and the extraction efficiency of CH_4 is affected by all three factors.

2.2. Coal Sample Preparation and Industrial Analysis. The experimental coal samples were taken from freshly exposed coal blocks in a mine in Shanxi Province. The coal was of poor rank, with a gas content between 14 and 18 m^3/t, implying a low gas drainage efficiency. To protect the experimental samples from oxidation during long-distance transportation, they were wrapped in plastic wrap and sent to the laboratory. After the original coal samples were pulverized into powder, they were screened through a standard sieve shaker, and 60−80 mesh coal samples larger than the 120 mesh were selected for industrial analysis. The results of the industrial analysis are shown in Table 1.

Table 1. Industrial Analysis Results

moisture/M_{ad}	ash/A_{ad}	volatile fraction/V_{ad}	fixed carbon/F_{ad}
1.50	12.06	9.14	77.30

2.3. Experimental Procedure. The detailed experimental steps are as follows.

1 The coal sample was ground to powder, placed it in the experimental tank, compacted it to ensure that the device is air-tight, and evacuated and degassed the experimental device.
2 The pressure-reducing valve of the CH_4 gas bottle was opened so that the coal sample in the adsorption tank adsorbs CH_4 gas until it is saturated.
3 CO_2 gas is injected into the adsorption tank to replace the CH_4 gas, and NaOH solution is used to collect and discharge CO_2 from the gas mixture.
4 Accurate, real-time monitoring data were collected until the end of the experiment.
5 The experimental parameters and the next set of experiments were modified according to the above steps.

https://doi.org/10.1021/acsomega.3c03016
ACS Omega 2023, 8, 28583−28591

The experimental design parameters are listed in Table 2.

Table 2. Experimental Design Parameters

CO_2 injection pressure /MPa	CH_4 adsorption equilibrium pressure /MPa	experimental temperature /°C	CO_2 gas temperature /°C
0.6	0.4	30	30
0.8	0.4	30	30
1.0	0.4	30	30

3. RESULTS AND DISCUSSION

3.1. Gas Migration Rate. The migration rate of the CH_4/CO_2 gas mixture in the coal seam during the experiment is determined by the following equation

$$v = \frac{l}{\Delta t} \quad (1)$$

where v is the migration rate of the gas mixture, cm/s; l is the distance between adjacent temperature monitoring points, cm; and Δt is the corresponding time difference between adjacent temperature monitoring points, s.

The experimental tank had three temperature monitoring points, each 10 cm apart, and the average migration rate of the gas mixture from temperature monitoring point T_1 to temperature monitoring points T_2 and T_3 was calculated.

The experiments to replace CH_4 with CO_2 were performed at pressures of 0.6, 0.8, and 1.0 MPa, and the migration rate of the gas mixture obtained from the experiments is shown in Figure 2.

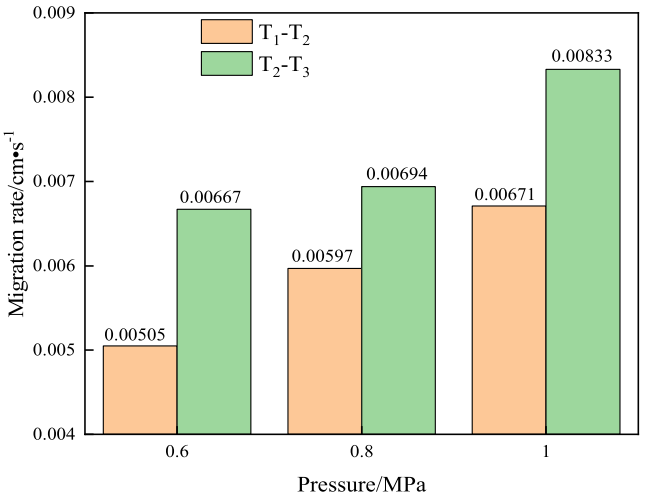

Figure 2. Gas migration rate under different gas injection pressures.

As shown in Figure 2, the gas injection pressure accelerates the rate of gas migration from T_1 to T_2 and from monitoring points T_2 to T_3 in all cases. After increasing the injection pressure from 0.6 to 0.8 MPa and then to 1.0 MPa, the migration rate increased from 0.005 to 0.00597 and 0.00671 cm/s for T_1−T_2, and from 0.0067 to 0.00694 and 0.00833 cm/s for T_2−T_3. The gas injection pressures of 0.8 and 1.0 MPa increased the transport rates from T_1 to T_2 by 18.2 and 32.9%, respectively, and from T_2 to T_3 by 4.1 and 24.9%, respectively, compared to those at 0.6 MPa. The average migration rate between T_2 and T_3 is higher than the average migration rate between T_1 and T_2 at the same gas injection pressure. Noticeably, when the gas injection pressure is increased, the migration rate of the gas mixture out of the coal seam is accelerated, implying that increasing the gas injection pressure can enhance the extraction of CH_4.

3.2. CH_4 Desorption Rate. The CH_4 desorption rate can describe CH_4 desorption at a specific point in the experiment to replace CH_4 with CO_2 and be used to determine how to increase the CH_4 extraction rate. The experiments to replace CH_4 with CO_2 were performed at 0.6, 0.8, and 1.0 MPa; the trend of the CH_4 desorption rate from the experiments is shown in Figure 3.

As shown in Figure 3, the trend of the gas desorption rate at different injection pressures comprises slowly decreasing, rapidly decreasing, and stable stages.

Stage I: the desorption rate of CH_4 decreased slowly. At the beginning of the experiment, the CH_4 content in the coal seam was high, and the amount of injected CO_2 was small, which had little influence on CH_4 desorption; accordingly, the trend is slowly downward. When the injection pressure was 0.6 MPa, the CH_4 desorption rate slowly decreased from 974.7 to 767.8 mL/min. The CO_2 percolation rate was maintained at approximately 10 mL/min. At 0.8 MPa, the CH_4 desorption rate decreased slowly from 976.3 to 832.9 mL/min, and the CO_2 percolation rate was maintained at approximately 18 mL/min. At an injection pressure of 1.0 MPa, the CH_4 desorption rate slowly decreased from 1010.1 to 954.9 mL/min, and the percolation rate of CO_2 was maintained at approximately 40 mL/min.

Stage II: the desorption rates of CH_4 and CO_2 after CO_2 broke through the coal seams sharply decreased and increased, respectively. This is attributable to the amount of CO_2 gas in the coal seam increasing and the amount of CH_4 gas decreasing, corresponding to increases and decreases in the partial pressures of CO_2 and CH_4, respectively, resulting in a decrease in the rate of CH_4 desorption and an increase in the rate of CO_2 percolation. At an injection pressure of 0.6 MPa, the CH_4 desorption rate decreased rapidly from 767.7 to 25.5 mL/min, whereas the CO_2 percolation rate rapidly increased to 580 mL/min. At an injection pressure of 0.8 MPa, the CH_4 desorption rate decreased rapidly from 832.9 to 130.6 mL/min, whereas the CO_2 percolation rate increased rapidly to 386 mL/min. At an injection pressure of 1.0 MPa, the CH_4 desorption rate decreased rapidly from 954.9 to 82.1 mL/min, and the CO_2 percolation rate increased rapidly to 622 mL/min.

Stage III: the desorption rate of CH_4 stabilized at approximately 30 mL/min, and the CO_2 percolation rate stabilized between 533.5 and 591.1 mL/min. At an injection pressure of 0.8 MPa, the desorption rate of CH_4 stabilized at approximately 20 mL/min, whereas the CO_2 percolation rate slightly decreased but remained at approximately 300 mL/min. At an injection pressure of 1.0 MPa, the desorption rate of CH_4 was stable at approximately 20 mL/min, whereas the CO_2 percolation rate decreased slowly and stabilized at approximately 400 mL/min at the end of the test.

Later in the experiment, the concentration of CH_4 gas at the outlet progressively decreased and gradually approached zero. The amounts of CO_2 injected and CO_2 discharged gradually approached each other until they were largely similar. Therefore, the penetration time of CO_2 can serve as an index for the rate at which the experiment proceeds, which is of great significance for measuring the repulsive effect of CO_2 on CH_4.

https://doi.org/10.1021/acsomega.3c03016
ACS Omega 2023, 8, 28583−28591

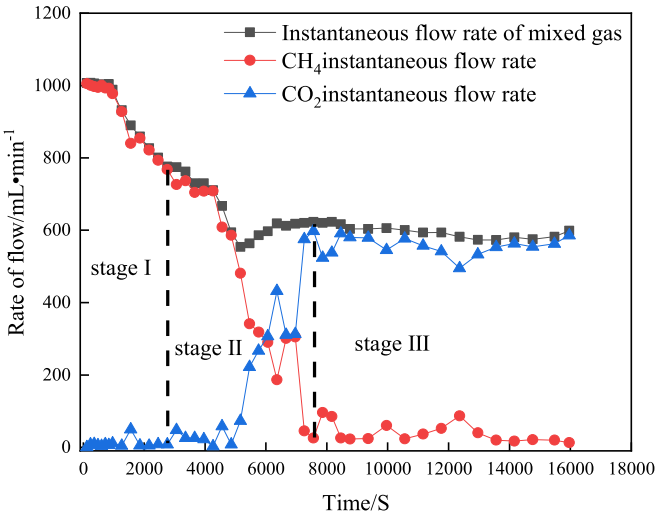

(a) Change in gas desorption rate at 0.6 MPa

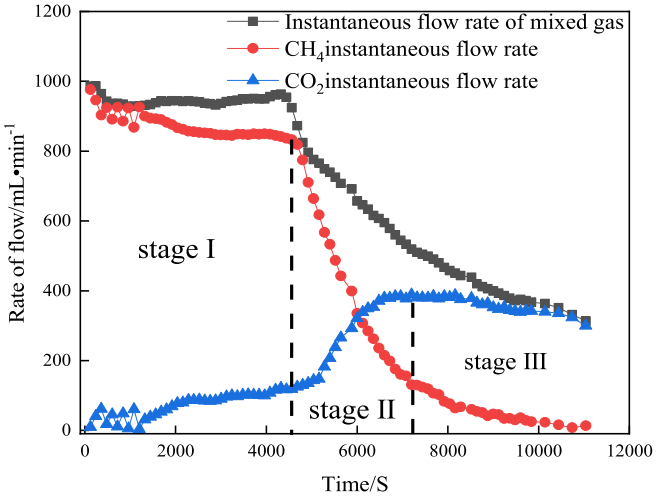

(b) Change in gas desorption rate at 0.8 MPa

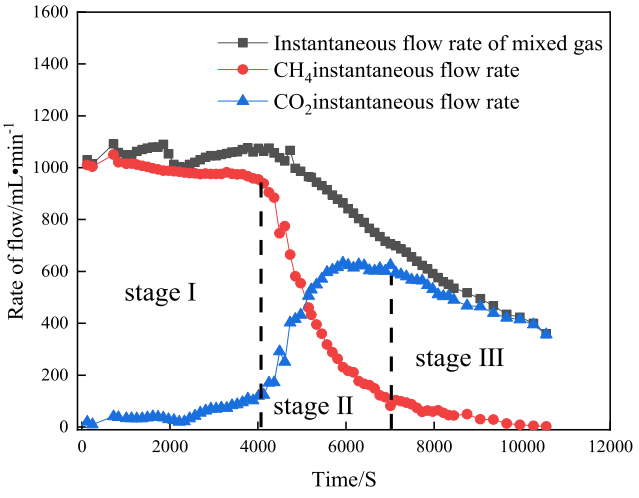

(c) Change in gas desorption rate at 1.0 MPa

Figure 3. Variation law of gas desorption rate under different gas injection pressures.

3.3. Effective Diffusion Coefficient of CH_4. Diffusivity is the ratio of CH_4 diffusion to the amount of CH_4 adsorbed by the coal body at any moment in the experiment, and the kinetic curve of CH_4 diffusion can serve as the curve of diffusivity with time. Equation 2 describes the single-pore diffusion model for gas diffusion in porous media.[37]

$$\frac{Q_t}{Q_\infty} = 1 - \frac{6}{\pi^2}\sum_{n=1}^{\infty}\frac{1}{n^2}\exp\left(-\frac{n^2\pi^2 D}{r_0^2}t\right) \quad (2)$$

where Q_t is the amount of gas diffusion at a given moment, mL/g; Q_∞ is the amount of gas adsorbed in the coal seam, mL/g; D is the diffusion rate, m^2/s; and r_0 is the coal particle radius, cm.

Equation 2 is a level addition and solution for $n = 1-\infty$, which is extremely difficult to solve when $n > 1$. Therefore, letting n be 1, it can be simplified to obtain eq 3.

$$\ln\left(1 - \frac{Q_t}{Q_\infty}\right) = -\frac{\pi^2 D}{r_0^2}t + \ln\frac{\pi^2}{6} \quad (3)$$

The above equation reveals that the slope of the tangent line at any point of the curve is $-D/r_0^2\cdot\pi^2$. Taking D/r_0^2 for the effective diffusion coefficient D_e, further processing can yield the effective diffusion coefficient D_e and time t between the curve. The effective diffusion coefficient D_e represents the degree of gas diffusion and reflects the diffusion capacity of the gas. Accurate calculations of the effective diffusion coefficient of CH_4 are useful for studying CH_4 diffusion in coal and estimating the amount of CH_4 loss. It can also be used to predict the occurrence of gas disasters.

Figure 4 shows the effective diffusion coefficient variation curve for different CO_2 injection pressures and the CH_4 effective diffusion coefficient and coal bed CH_4 gas pressure variation curves at 0.6 MPa.

Figure 4 shows that the pattern of change in the effective diffusion coefficient comprises a rapidly increasing first stage, a rapidly decreasing second stage, and a final stabilization stage.

First stage: the CH_4 gas in the fissure in the coal seam has been adsorbed in equilibrium, the CH_4 gas pressure in the coal seam is high, the injected CO_2 gas starts to carry free-state CH_4 out, and the CH_4 gas pressure exhibits a slow decreasing trend.

https://doi.org/10.1021/acsomega.3c03016
ACS Omega 2023, 8, 28583−28591

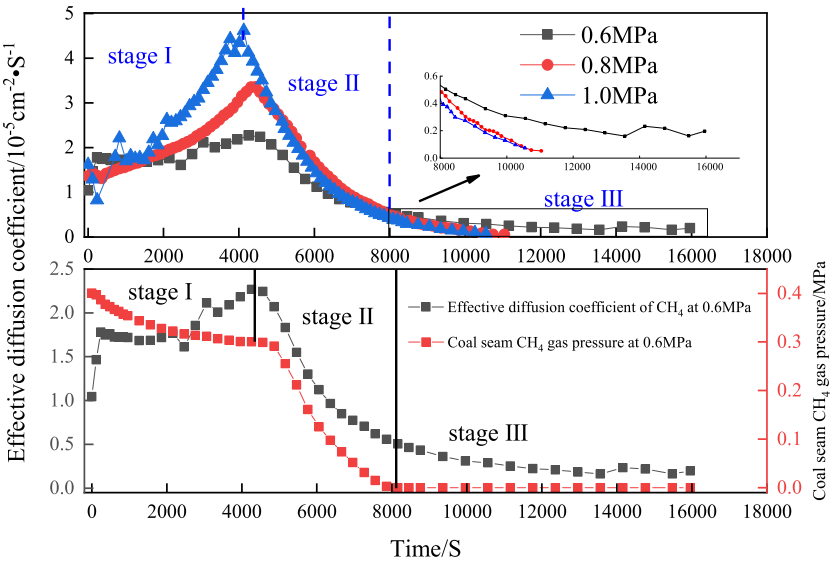

Figure 4. Variation curves of effective diffusion coefficient with different CO_2 injection pressures and CH_4 effective diffusion coefficient and coal bed CH_4 gas pressure at 0.6 MPa.

From a macroscopic point of view, the CO_2 concentration differs with location in the coal seam fracture, and these differences result in the gradual increase in the effective diffusion coefficient of CO_2. Microscopic analysis reveals that the CO_2 injection at the beginning of the experiment is small, the coal seam has not yet adsorbed CO_2, and the displacement of CO_2 and CH_4 in the pores positively affects diffusion.

Second stage: the free-state CH_4 in the pores has escaped, and CO_2 molecules start to compete with CH_4 molecules for adsorption at the adsorption sites inside the coal seam. Moreover, the adsorbed CH_4 is replaced by the injected CO_2. An exothermic CO_2 adsorption process occurs in the coal seam, resulting in the CH_4 gas molecules absorbing heat, and the adsorbed CH_4 molecules in the pores start to desorb and escape from the coal seam. Meanwhile, the CH_4 gas pressure in the coal seam drops rapidly. After CO_2 penetrates the coal seam, the partial pressure of CO_2 gas in the coal seam increases rapidly, the coal seam pores adsorb numerous CO_2 molecules, and the amount of CO_2 in the pores increases. Due to the replacement by CO_2 gas, the CH_4 content in the coal seam decreases, the CH_4 concentration gradient in the pores decreases, the diffusion effect begins to weaken, and the effective diffusion coefficient of CH_4 begins to decrease.

Third stage: most of the CH_4 gas in the coal seam has been replaced and escaped, the CH_4 gas pressure in the coal seam is stable at its lowest, the coal seam has adsorbed a large amount of CO_2 gas, and the pores are largely saturated with CO_2 gas molecules. Subsequently, the concentration of CH_4 gas in the pore is very low; the CH_4 diffusion is very small, which has little influence on the diffusion of CH_4; and the effective diffusion coefficient tends to be stable.

The effective diffusion coefficient becomes larger when the gas injection pressure increases. After the injection pressure increases from 0.6 to 0.8 MPa and then to 1.0 MPa, the maximum value of the effective diffusion coefficient increases from 2.3×10^{-5} to 3.4×10^{-5} and 4.6×10^{-5} cm^2/s. Increasing the gas injection pressure can make CH_4 diffuse more fully in the coal seam, so the higher the gas injection pressure is at the later stage of the experiment, the lower the value of its effective diffusion coefficient.

3.4. Coal Seam Permeability Variation. The pumping injection was maintained throughout the experiment, which affected the pore structure of the coal seam and constantly changed it; thus, the permeability of the experimental coal body changes dynamically; eq 4 is used to calculate the permeability.[38]

$$K = \frac{2QP\mu L}{A(P_a^2 - P_b^2)} \tag{4}$$

where K is the permeability, 10^{-9} μm^2; P is the standard atmospheric pressure, 1.01×10^5 Pa; Q is the flow rate, mm^3/s; P_a is the inlet gas pressure, MPa; P_b is the outlet gas pressure, MPa; L is the specimen size, mm; A is the specimen cross-sectional area, mm^2; and μ is the dynamic viscosity of CO_2, μPa s.

The pattern of coal seam permeability change under the three experimental conditions is shown in Figure 5.

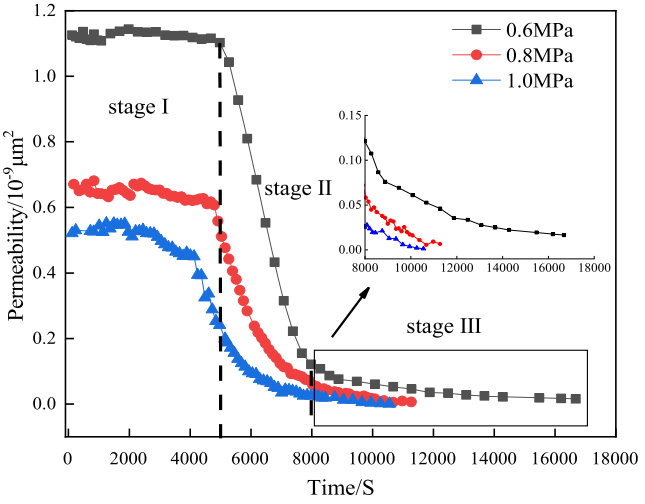

Figure 5. Variation in permeability with time under different pressures.

https://doi.org/10.1021/acsomega.3c03016
ACS Omega 2023, 8, 28583−28591

As can be seen from Figure 5, the trend of permeability change is the same for the three groups of experimental coal seams.

First stage: the permeability decreased slowly due to the increase in the amount of gas in the coal seam after a small amount of CO_2 was injected at the beginning of the experiment. The permeability of the three experimental coal seams was reduced from 1.13×10^{-9} to 1.10×10^{-9} μm^2, 0.68×10^{-9} to 0.62×10^{-9} μm^2, and 0.52×10^{-9} to 0.48×10^{-9} μm^2.

Second stage: the permeability decreases sharply because CH_4 continues to desorb and escape from the coal seam as the experiment progresses, and the amount of CO_2 gas adsorbed in the coal seam increases, leading to an increase in replacement adsorption−desorption. Moreover, the continuous adsorption−desorption causes the pores of the coal seam to expand and contract. As a large amount of CH_4 gas desorption escapes from the coal seam, the adsorption of CO_2 by the coal seam begins to dominate. This increases the amount of gas adsorbed in the pores of the coal seam, which is not conducive to seepage, so the permeability decreases. The permeability of the three experimental coal seams was reduced from 1.13×10^{-9} to 0.12×10^{-9} μm^2, 0.62×10^{-9} to 0.05×10^{-9} μm^2, and 0.48×10^{-9} to 0.03×10^{-9} μm^2.

Third stage: the CO_2 gas molecules in the pores of the coal seam were gradually saturated, largely reaching the adsorption equilibrium. As the experiment progresses, the overall temperature of the coal sample in the adsorption tank increases, and the thermal effect of the coal seam influences the change process of the pores and cracks in the coal seam. Some pores and cracks change from the expanded state to the closed state, the deformation of the pores reaches the maximum limit of elastic deformation, and seepage is primarily stable, so the permeability tends to be stable.

3.5. Effectiveness of Coalbed Methane Extraction.

(1) Amount of desorbed CH_4: the experiments were performed at 0.6, 0.8, and 1.0 MPa to replace CH_4 with CO_2, and the trend of CH_4 desorption during the experiments is shown in Figure 6.

As can be seen from Figure 6, the patterns of CH_4 desorption at each injection pressure become largely similar as the experiment progresses, with CH_4 continuously escaping from the coal seam as the experiment progresses. Furthermore, the amount of desorbed CH_4 continuously increases before stabilizing at the end of the experiment.

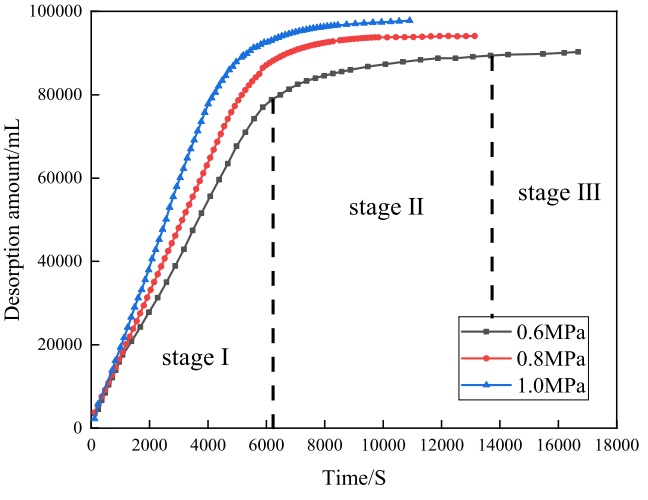

Figure 6. Variation trend of CH_4 desorption under different gas injection pressures.

At the beginning of the experiment, the desorption rate of CH_4 was high, and the replacement rate was highest. The desorbed CH_4 gas in the pores of the coal seam was mainly free CH_4, which was relatively easy to replace.

Halfway into the experiment, the rate of the CH_4 desorption volume increase was low, and the CH_4 desorption rate was low. This is mainly because most of the CH_4 gas in the coal seam had been expelled from the coal seam, and replacing and repelling the remaining CH_4 gas in the coal seam is difficult.

The CH_4 desorption volume increased from 90.2 to 94.1 and 97.8 L after the gas injection pressure was increased from 0.6 to 0.8 MPa and then to 1.0 MPa, which were 1.9 and 3.4% higher than that at 0.6 MPa. A higher gas injection pressure simultaneously corresponds to more CH_4 desorption.

(2) CO_2 storage capacity: the experiments were conducted at 0.6, 0.8, and 1.0 MPa to replace CH_4 with CO_2, and the trend of the CH_4 storage capacity during the experiments is shown in Figure 7.

It can be seen from Figure 7 that the trend of CO_2 sequestration in the coal seams is similar to that of CH_4 desorption under the three experimental conditions. At the beginning of the experiment, the concentration of CO_2 gas at the exit was zero, which indicates that all the injected CO_2 gas in the coal seam was absorbed, and the CO_2 storage increased rapidly. As CO_2 began to rush out of the coal seam, the concentration of CO_2 gas at the exit increased rapidly, and most of the injected CO_2 gas escaped with the gas flow. In contrast, the growth rate of CO_2 storage reduced before finally stabilizing. During the experiment, a higher gas injection pressure corresponded to greater CO_2 storage in the coal seam because the higher the gas injection pressure is, the more CO_2 gas molecules enter the pores of the coal seam and fully contact with them. This increases the amount of CO_2 entering the tiny pores of the coal seam and enhances the displacement between CO_2 and CH_4 molecules in the pores of the coal seam, which leads to an increase in the CH_4 gas replaced and amount of CO_2 adsorbed in the coal seam.

When the injected CO_2 starts to break through the coal seam and escape, the amount of sequestered CO_2 varies with injection pressure. At 0.6 MPa, the CO_2 breakthrough time was 4560 s, and the CO_2 storage capacity was 146.0 L. At 0.8 MPa, the CO_2 breakthrough time was 4440 s, and the CO_2 storage capacity was 193.5 L. At 1.0 MPa, the CO_2 breakthrough time was 3890 s, and the CO_2 storage capacity was 204.4 L. At the end of the experiment, the CO_2 storage capacities were as follows: the amount of CO_2 sequestered in the coal seam was 269.2, 274.2, and 322.8 L for injection pressures of 0.6, 0.8, and 1.0 MPa, respectively. Notably, the amount of CO_2 sequestered in the coal seam increased when the CO_2 injection pressure was increased.

(3) Extraction efficiency: to further analyze the effect of replacement of CH_4 by CO_2, the CH_4 extraction efficiency was calculated using the following equation

$$E = \frac{Q_a(CH_4)}{Q_b(CH_4)} \times 100\% \quad (5)$$

https://doi.org/10.1021/acsomega.3c03016
ACS Omega 2023, 8, 28583−28591

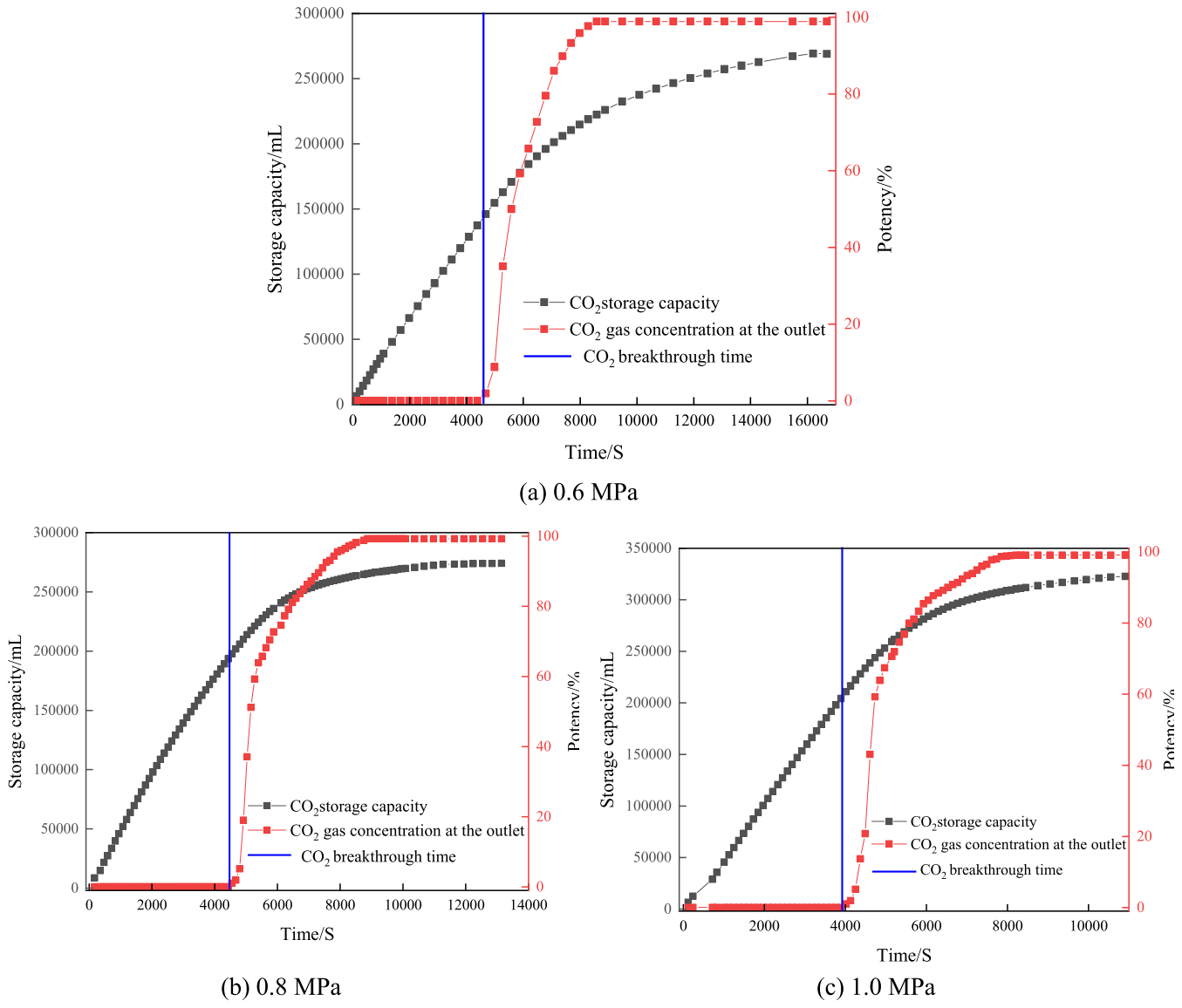

Figure 7. Desorption efficiency of CH_4 under different gas injection pressures.

where E is the CH_4 extraction efficiency, %; Q_a (CH_4) is the amount of CH_4 desorbed from the coal seam, L; and Q_b (CH_4) is the amount of original CH_4 from the coal seam, L.

The CH_4 extraction efficiency during the experiments at different pressures is shown in Figure 8.

As can be seen from Figure 8, after the CO_2 injection pressure was increased from 0.6 to 0.8 MPa and then to 1.0 MPa, the CH_4 extraction efficiency increased from 76.9 to 80.2 and 82.9%. Compared with that at the injection pressure of 0.6 MPa, the extraction efficiency increased by 4.3 and 7.8% when the injection pressure was 0.8 and 1.0 MPa, respectively. The coal seam pressure was in a state of dynamic change during the experiment, which affected the pore structure of the coal seam. The higher the CO_2 injection pressure is, the greater the change in the coal seam pressure, and the more its pore structure is affected. Therefore, more CH_4 gas was desorbed from the coal seam, and the CH_4 extraction efficiency increased. When the CO_2 injection pressure is increased, the replacement effect of CO_2 on CH_4 in the coal seam is enhanced, so increasing the CO_2 injection pressure improves the CH_4 extraction effect in the coal seam.

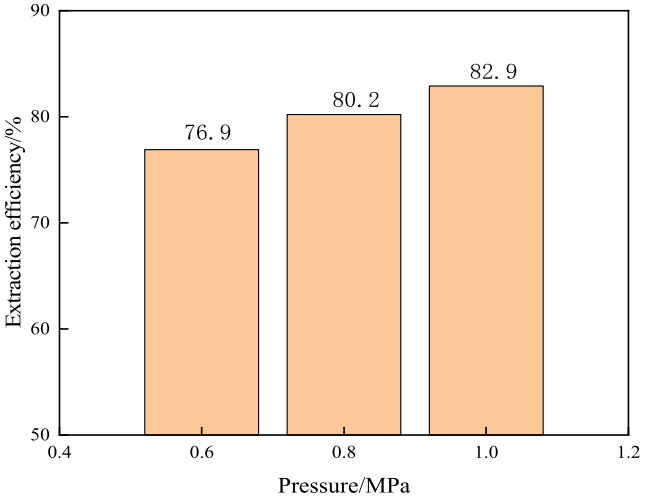

Figure 8. Extraction efficiency of CH_4 under different gas injection pressures.

https://doi.org/10.1021/acsomega.3c03016
ACS Omega 2023, 8, 28583−28591

4. CONCLUSIONS

Herein, an experimental study on the replacement of CH_4 under different CO_2 injection pressures was conducted using the CO_2 replacement CH_4 experimental platform, and the gas transport characteristics and CBM extraction effects during the experimental process were analyzed. The main conclusions are as follows.

1 The gas migration rate accelerated when the gas injection pressure was increased. After the gas injection pressure was increased from 0.6 to 0.8 MPa and then to 1.0 MPa, the migration rates from monitoring points T_1 to T_2 were 0.005, 0.00597, and 0.00671 cm/s, respectively, whereas the migration rates from monitoring points T_2 to T_3 were 0.0067, 0.00694, and 0.00833 cm/s, respectively. Comparisons of the migration rates between adjacent monitoring points revealed that they accelerated with the increase in gas injection pressure. As the gas injection pressure increases, the rate of gas migration out of the coal seam is accelerated, and increasing the gas injection pressure can improve the CH_4 extraction.

2 The change trend of the gas desorption rate under different injection pressures can be divided into slow decline, sharp decline, and stability stages with the increase in injection pressure. Moreover, the CO_2 breakthrough time is increased, and the change in the CH_4 desorption rate is accelerated. The higher the gas injection pressure is, the larger the maximum effective diffusion coefficient. Moreover, after increasing the gas injection pressure from 0.6 to 0.8 MPa and then to 1.0 MPa, the maximum effective diffusion coefficient increases from 2.3×10^{-5} to 3.4×10^{-5} and 4.6×10^{-5} cm^2/s. The change pattern of the coal seam permeability can also be divided into three stages: slowly decreasing, sharply decreasing, and stable. The permeability change pattern can also be divided into slow decline, sharp decline, and stability stages, and increasing the gas injection pressure can accelerate the change in permeability.

3 As the gas injection pressure increases, the CH_4 desorption volume, CO_2 sequestration volume in the coal seam, and CH_4 extraction efficiency increase. After the injection pressure was increased from 0.6 to 0.8 MPa and then to 1.0 MPa, the CH_4 desorption volume increased from 90.2 to 94.1 and 97.8 L, whereas the CO_2 sequestration volume in the coal seam increased from 269.2 to 273.2 and 322.8 L. In contrast, the CH_4 extraction efficiency increased from 76.9 to 80.2 and 82.9%.

AUTHOR INFORMATION

Corresponding Author

Baoshan Jia − *College of Safety Science and Engineering, Liaoning Technical University, Fuxin, Liaoning 123000, China; Key Laboratory of Mine Thermodynamic Disasters and Control of Ministry of Education, Liaoning Technical University, Huludao, Liaoning 125105, China;* orcid.org/0009-0001-2267-5952; Email: jiabaoshan@Intu.edu.cn

Authors

Zhihao Fu − *College of Safety Science and Engineering, Liaoning Technical University, Fuxin, Liaoning 123000, China; Key Laboratory of Mine Thermodynamic Disasters and Control of Ministry of Education, Liaoning Technical University, Huludao, Liaoning 125105, China*

Yanming Wang − *College of Safety Science and Engineering, Liaoning Technical University, Fuxin, Liaoning 123000, China; Key Laboratory of Mine Thermodynamic Disasters and Control of Ministry of Education, Liaoning Technical University, Huludao, Liaoning 125105, China*

Weipeng Tian − *College of Safety Science and Engineering, Liaoning Technical University, Fuxin, Liaoning 123000, China; Shanxi Coal Import & Export Group Zuoyun Donggucheng Coal Company Limited, Datong, Shanxi 037100, China*

Complete contact information is available at: https://pubs.acs.org/10.1021/acsomega.3c03016

Notes

The authors declare no competing financial interest.

ACKNOWLEDGMENTS

We sincerely thank the editors and anonymous reviewers for improving the quality of this manuscript, as well as MJEditor (www.mjeditor.com) for providing English editing services.

REFERENCES

(1) *BP Energy Outlook*, 2019 ed.: London, United Kingdom, 2019.

(2) Orr, F. M. Onshore Geologic Storage of CO_2[J]. *Science* **2009**, *325*, 1656−1658.

(3) Anwar, M. N.; Fayyaz, A.; Sohail, N. F.; Khokhar, M. F.; Baqar, M.; Yasar, A.; Rasool, K.; Nazir, A.; Raja, M.; Rehan, M.; et al. CO_2 utilization: turning greenhouse gas into fuels and valuable products. *J. Environ. Manage.* **2020**, *260*, 110059.

(4) Opara, A.; Adams, D. J.; Free, M. L.; McLennan, J.; Hamilton, J. Microbial production of methane and carbon dioxide from lignite, bituminous coal, and coal waste materials. *Int. J. Coal Geol.* **2012**, *96*−*97*, 1−8.

(5) Oreggioni, G. D.; Luberti, M.; Tassou, S. A. Agricultural greenhouse CO_2 utilization in anaerobic-digestion-based biomethane production plants: a techno-economic and environmental assessment and comparison with CO_2 geological storage. *Appl. Energy* **2019**, *242*, 1753−1766.

(6) Liu, Y.; Rui, Z. A storage-driven CO_2 EOR for a net-zero emission target. *Engineering* **2022**, *18*, 79−87.

(7) Fan, C.; Elsworth, D.; Li, S.; Zhou, L.; Yang, Z.; Song, Y. Thermo-hydro-mechanical- chemical couplings controlling CH_4 production and CO_2 sequestration in enhanced coalbed methane recovery. *Energy* **2019**, *173*, 1054−1077.

(8) Qin, L.; Ma, C.; Li, S.; Lin, H.; Ding, Y.; Liu, P.; Wang, P.; Gao, Z. Liquid Nitrogen's Effect on the Mechanical Properties of Dried and Water-Saturated Frozen Coal. *Energy Fuels* **2022**, *36*, 1894−1903.

(9) Qin, L.; Wang, W.; Lin, H.; Liu, P.; Long, H.; Yang, E.; Lin, S. Temperature evolution and freeze−thaw characteristics of water-saturated-dried coal samples during low-temperature freeze−thaw process. *Fuel* **2022**, *324*, 124689.

(10) Du, Y. *ScCO_2 Experimental Study on Mineral Geochemistry and Reservoir Structure Response of Injected Coal Seam*; China University of Mining and Technology, 2018.

(11) Rathi, R.; Lavania, M.; Singh, N.; Manab Sarma, P.; Kishore, P.; Hajra, P.; Lal, B. Evaluating indigenous diversity and its potential for microbial methane generation from thermogenic coal bed methane reservoir. *Fuel* **2019**, *250*, 362−372.

(12) Mazzotti, M.; Pini, R.; Storti, G. Enhanced coalbed methane recovery. *J. Supercrit. Fluids* **2009**, *47*, 619−627.

(13) Yu, S.; Bo, J.; Meijun, Q. Molecular Dynamic Simulation of Self- and Transport Diffusion for $CO_2/CH_4/N_2$in Low-Rank Coal Vitrinite. *Energy Fuels* **2018**, *32*, 3085−3096.

(14) Zeng, Q.; Wang, Z.; Liu, L.; Ye, J.; McPherson, B. J.; McLennan, J. D. Modeling CH_4 Displacement by CO_2 in Deformed Coalbeds during Enhanced Coalbed Methane Recovery. *Energy Fuels* **2018**, *32*, 1942−1955.
(15) Aminu, M. D.; Ali Nabavi, S.; Rochelle, C. A.; Manovic, V. A review of developments in carbon dioxide storage. *Appl. Energy* **2017**, *208*, 1389−1419.
(16) Xiao, B.; Liu, S.; Li, Z.; Ran, B.; Ye, Y.; Yang, D.; Li, J. Geochemical characteristics of marine shale in the Wufeng Formation−Longmaxi Formation in the northern Sichuan Basin, South China and its implications for depositional controls on organic matter. *J. Petrol. Sci. Eng.* **2021**, *203*, 108618.
(17) Yu, H.; Jiang, Q.; Song, Z.; Ma, Q.; Yuan, B.; Xiong, H. The economic and CO_2 reduction benefits of a coal-to-olefins plant using a CO_2-ECBM process and fuel substitution. *RSC Adv.* **2017**, *7*, 49975−49984.
(18) Fujioka, M.; Yamaguchi, S.; Nako, M. CO_2-ECBM field tests in the Ishikari Coal Basin of Japan. *Int. J. Coal Geol.* **2010**, *82*, 287−298.
(19) White, C. M.; Smith, D. H.; Jones, K. L.; Goodman, A. L.; Jikich, S. A.; LaCount, R. B.; DuBose, S. B.; Ozdemir, E.; Morsi, B. I.; Schroeder, K. T. Sequestration of carbon dioxide in coal with enhanced coalbed methane recovery: A review. *Energy Fuels* **2005**, *19*, 659−724.
(20) Yu, H.; Yuan, J.; Guo, W.; Cheng, J.; Hu, Q. A preliminary laboratory experiment on coalbed methane displacement with carbon dioxide injection. *Int. J. Coal Geol.* **2008**, *73*, 156−166.
(21) Prusty, B. K. Sorption of methane and CO_2 for enhanced coalbed methane re-covery and carbon dioxide sequestration. *J. Nat. Gas Chem.* **2008**, *17*, 29−38.
(22) Bai, G.; Su, J.; Zhang, Z.; Lan, A.; Zhou, X.; Gao, F.; Zhou, J. Effect of CO_2 injection on CH_4 desorption rate in poor permeability coal seams: An experimental study. *Energy* **2022**, *238*, 121674.
(23) Tu, B.; Xie, C.; Li, W.; et al. Study on the adsorption/desorption patterns of CO_2, CH_4 and N_2 by coal seams. *Coal Sci. Technol.* **2012**, *40*, 70−72.
(24) Tang, S.; Tang, D.; Yang, Q. The variation law of gas fraction in isothermal adsorption-desorption of binary gases. *J. China Univ. Min. Technol.* **2004**, *04*, 86−90.
(25) Long, H.; Lin, H. F.; Yan, M.; et al. Adsorption and diffusion characteristics of CH_4, CO_2, and N_2 in micropores and mesopores of bituminous coal: Molecular dynamics. *Fuel* **2021**, *292*, 120268.
(26) Liu, Y. W.; Liu, M. J. Effect of particle size on the variability of gas desorption diffusion of soft and hard coal grains. *J. Coal* **2015**, *40*, 579−587.
(27) An, F. H.; Jia, H. F.; Liu, J. Research on gas diffusion model based on coal pore composition. *J. Rock Mech. Eng.* **2021**, *40*, 987−996.
(28) Yang, H. M.; Liang, L. H.; Feng, C. Y.; et al. Influence of gas injection pressure on displacement effect of gas from different injection sources. *Chin. J. Saf. Sci.* **2017**, *27*, 7.
(29) Wu, D.; Liu, X. Y.; Sun, K. M.; et al. Experimental study on mechanical properties and permeability of coal and rock containing CH_4 after CO_2 injection. *Chin. J. Saf. Sci.* **2015**, *25*, 5.
(30) Yang, T. H.; Chen, L. W.; Yang, H. M.; et al. Experimental study on the transformation process of the mechanism of carbon dioxide injection to promote coal seam gas drainage. *J. Northeast. Univ., Nat. Sci.* **2020**, *41*, 623−628.
(31) Jing, J. J. *Experimental Study on the Influence of Coal Water Content on CO_2 Displacement of CH_4*; Taiyuan University of Technology: Taiyuan, 2016.
(32) Zhou, X. H.; Jiang, P. F.; Bai, G.; et al. Test and analysis of replacement efficiency of CO_2 displacing CH_4. *Chin. J. Saf. Sci.* **2020**, *30*, 6.
(33) Meng, J. Q.; Li, S. C.; Niu, J. X.; Meng, H. X.; Zhong, R. Q.; Zhang, L. F.; Nie, B. Effects of moisture on methane desorption characteristics of the Zhaozhuang coal: experiment and molecular simulation. *Environ. Earth Sci.* **2020**, *79*, 44.
(34) Wu, S.; Guo, Y. Discussion on the mechanism of gas injection to develop coalbed methane. *J. Taiyuan Univ. Technol.* **2000**, *4*, 361−363.
(35) Mazumder, S.; Wolf, K. H. A. A.; van Hemert, P.; Busch, A. Laboratory Experiments on Environmental Friendly Means to Improve Coalbed Methane Production by Carbon Dioxide/Flue Gas Injection. *Transp. Porous Media* **2008**, *75*, 63−92.
(36) Li, J.; Zhang, L.; Xue, J.; Zhang, C.; Huang, M. CO_2 in gas injection displacementReplacement of coal body CH_4 Behavior characteristics. *J. Coal Sci.* **2021**, *46*, 385−395.
(37) Liu, T.; Lin, B. Q.; Fu, X. H.; Gao, Y.; Kong, J.; Zhao, Y.; Song, H. Experimental study on gas diffusion dynamics in fractured coal: a better understanding of gas migration in in-situ coal seam. *Energy* **2020**, *195*, 117005.
(38) Zhang, Z. M.; Liang, W. G. Experimental study on the influence of adsorbed gas on coal permeability. *J. Taiyuan Univ. Technol.* **2013**, *44*, 356−360.

https://doi.org/10.1021/acsomega.3c03016
ACS Omega 2023, 8, 28583−28591